

Document downloaded from:

<http://hdl.handle.net/10251/120634>

This paper must be cited as:

Mohamed Mohamed-Hicho, N.; Antonino Daviu, E.; Cabedo Fabres, M.; Ferrando Bataller, M. (2018). Designing Slot Antennas in Finite Platforms using Characteristic Modes. IEEE Access. 6:41346-41355. <https://doi.org/10.1109/ACCESS.2018.2847726>



The final publication is available at

<http://doi.org/10.1109/ACCESS.2018.2847726>

Copyright Institute of Electrical and Electronics Engineers

Additional Information

(c) 2018 IEEE. Personal use of this material is permitted. Permission from IEEE must be obtained for all other users, including reprinting/ republishing this material for advertising or promotional purposes, creating new collective works for resale or redistribution to servers or lists, or reuse of any copyrighted components of this work in other works.

# Designing Slot Antennas in Finite Platforms using Characteristic Modes

Nora Mohamed Mohamed-Hicho<sup>1</sup>, Student Member, IEEE, Eva Antonino-Daviu<sup>1</sup>, Member, IEEE, Marta Cabedo-Fabrés<sup>1</sup>, Member, IEEE, Miguel Ferrando-Bataller<sup>1</sup>, Member, IEEE

<sup>1</sup>Institute of Telecommunications and Multimedia Applications (iTEAM), Edificio 8G, Universitat Politècnica de València, Camino de Vera s/n, 46022, Valencia, Spain

Corresponding author: Nora Mohamed Mohamed-Hicho (e-mail: nomomo@upvnet.upv.es).

This work was supported by Spanish Ministry of Economy and Competitiveness under project TEC2016-78028-C3-3.

**ABSTRACT** In this paper, the application of the Theory of Characteristic Modes for the design of narrow-in-width open slot antennas embedded in finite platforms is investigated. Purely magnetic and electric Characteristic Modes (CM) of a slot etched in both an infinite and a finite ground plane are analyzed, with the aim to provide a physical understanding of the slot behavior and its interaction with the metallic ground plane. Instead of traditional CM analysis, an alternative approach is proposed, which consists in dividing the design procedure into the separate and complementary analysis of purely magnetic and electric CM. Based on this analysis, some guidelines for the design of open slot antennas are provided, and a simple and compact narrow-in-width wideband open slot antenna is designed. Simulations and measurements are presented for the optimized slot antenna, showing an impedance bandwidth of 47.48% with a very stable radiation pattern.

**INDEX TERMS** Characteristic Modes, Magnetic modes, Excitation of Characteristic Modes, Slot Antenna, Aperture Antenna, Antenna Design.

## I. INTRODUCTION

The Theory of Characteristic Modes (TCM), defined by Garbacz, Harrington and Mautz [1]-[3] nearly fifty years ago, has become very popular in the last years, as it has proven to be really effective for the systematic design of antennas in several modern applications [4]-[19]. The impressive success of the TCM in modern systems lies in the fact that it provides very interesting physical insight into the potential radiating characteristics of an antenna, prior to the selection of the excitation, as Characteristic Modes (CM) are intrinsic to the radiating structure and are computed numerically in absence of excitation. This fact paves the way for a systematic design methodology, in contrast to automated optimization methods or trial-and-error approaches, which do not usually bring any physical understanding about the antenna behavior.

From the first antenna applications of the TCM reviewed in [4], the rise of the computing power during the last decades has brought the possibility to extend the use of the TCM to modern applications, including design of small antennas [6] [7], vehicle mounted antennas [8][9], handset and MIMO antennas [10]-[13], wideband antennas [14],

dielectric antennas [15]-[16], and, more recently, nanoantennas [17] or metasurfaces [18][19], among others.

However, although the TCM has attracted great interest for many applications, its use for systematic design of slot antennas has been limited so far.

CM can be computed for slot or aperture problems by considering a weighted eigenvalue equation based on the admittance operator, as proven in [20], where the first CM analysis of an aperture based on equivalent magnetic currents is presented. Moreover, the CM of infinite slots in conducting planes excited by TM and TE plane waves were analyzed and computed in [21]-[23], whereas the characteristic magnetic currents of a rectangular aperture in an infinite perfectly conducting ground plane were obtained in [24]. However, the CM analysis in all these cases is restricted to infinite ground planes and cannot be directly applied to slots etched in finite ground planes or finite platforms, which are the scope of this paper.

In planar antenna design, the addition of narrow slots is a well-known technique for size reduction [25], creation of extra resonances [26][27], production of dual or circular polarization [28][29], and generation of band-notch effects

[30]. In general, a first approach for the systematic design of a slot antenna embedded in a metallic patch would be based on the classical formulation of the TCM based on purely electric current modes ( $J_n$ ), as in [31]-[35].

The electric formulation of the TCM brings valuable information when the electric CM of the metallic patch containing the slot are directly excited (e.g. through a feeding probe, microstrip or CPW line). In this case, resonances and anti-resonances of the input impedance are determined by these electric CM [5], whereas the slot acts simply as a coupled or parasitic element whose effect on input impedance and polarization can be derived straightforwardly by classical TCM analysis.

Conversely, when the excitation is applied to the slot, the resonances and anti-resonances of the input impedance are mainly determined by the magnetic CM of the slot, and the purely electrical formulation of TCM fails to provide a comprehensive explanation of the antenna behavior. However, in addition to the slot geometry, dimensions of the ground plane also exert a significant influence on the resultant radiation pattern, so the ground plane effect should be considered in the analysis.

An alternative approach for open slot antenna analysis could be based on the inclusion of some dielectric material in the slot and the computation of magnetic and electric CM using the method proposed by Chang and Harrington for material bodies [36], using the Poggio–Miller–Chang–Harrington–Wu–Tsai (PMCHWT) formulation. However, it has been shown that this formulation and similar ones [37] lead to the apparition of spurious modes, the so-called “non-physical modes” [38][39]. Interpretation of the nature of these non-physical modes has been a controversial topic lately. However, in [40] it is shown that these modes have a significant contribution to the inner field when the excitation source is located within the dielectric body, so these modes should be taken into account and cannot be discarded, as is a common practice.

This paper proposes an alternative hybrid method based on the combination of purely magnetic and electric modal analysis for a narrow-in-width rectangular slot antenna embedded in a finite ground plane. Moreover, some design guidelines are provided to improve the interaction between the slot and the finite ground plane modes. For the sake of brevity, only the case of a center-fed open slot antenna is considered in the paper. However, the proposed method and design procedure can be extended to any type of excitation (e.g. off-centered slot, double-fed slot, etc.).

The structure of the paper is the following: Section II presents the magnetic CM of a rectangular slot in an infinite ground plane. Section III analyzes the effect of the ground plane size and Section IV discusses the application of magnetic and electric CM to the design of slot antennas in finite ground planes and provides design guidelines for an appropriate selection of the ground plane size. Section V proposes a very simple open slot antenna design with

enhanced bandwidth, based on the results of previous sections. Finally, the main conclusions of the paper are summarized.

## II. MAGNETIC MODAL ANALYSIS OF A SLOT IN AN INFINITE GROUND PLANE

Let us consider an infinite ground plane with an etched rectangular slot of 82 mm x 3 mm (see Fig. 1, where  $L_h=L_v=\infty$ ). As commented previously, equivalent magnetic currents can be used to compute the CM of the structure by considering an admittance operator and the following weighted eigenvalue equation [20]:

$$B(M_n) = b_n G(M_n) \quad (1)$$

where  $b_n$  are the real magnetic eigenvalues,  $M_n$  are the magnetic characteristic currents, and  $G$  and  $B$  are the real and imaginary parts of the admittance operator  $Y$ :

$$Y = G + jB \quad (2)$$

Fig. 2 depicts the variation with frequency of the real eigenvalues for the first three purely magnetic modes  $M_n$  of the slot, obtained with FEKO. A magnetic mode is at resonance when its associated real eigenvalue is equal to zero ( $b_n = 0$ ). As observed, the resonances of the first three magnetic CM of the slot occur at 1.67 GHz, 3.46 GHz and 5.25 GHz, corresponding to approximate slot lengths ( $L_s$ ) of  $\lambda/2$ ,  $\lambda$  and  $3\lambda/2$ , respectively. As seen, the magnetic resonant modes show inductive behavior at low frequencies, when the real magnetic eigenvalue is less than zero ( $b_n < 0$ ) and capacitive behavior after resonance ( $b_n > 0$ ). The simulated 3D radiation patterns at resonance are also presented in Fig. 2 for the first three magnetic modes.

Fig. 3 shows the magnetic current distribution in the slot for these first three modes at their respective resonance frequency. For a better understanding of the magnetic current flow, black arrows have been overlaid on the figure. As observed, this magnetic current distribution is equivalent to the electric current distribution associated to a dipole with the same dimensions [5], as a result of the duality between the magnetic CM of a slot and the well-known electric CM of a dipole.

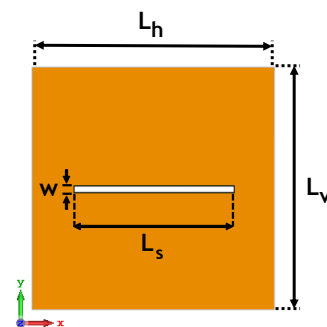
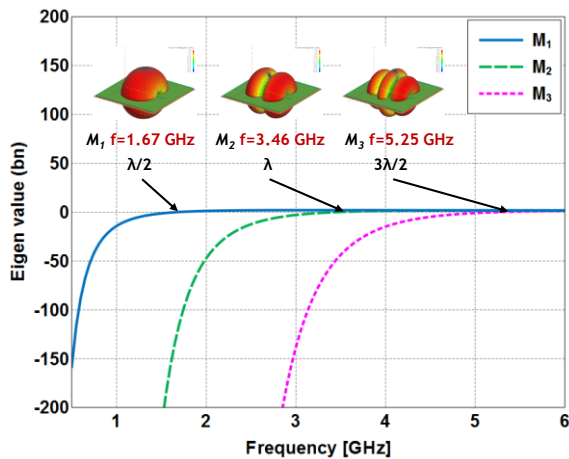
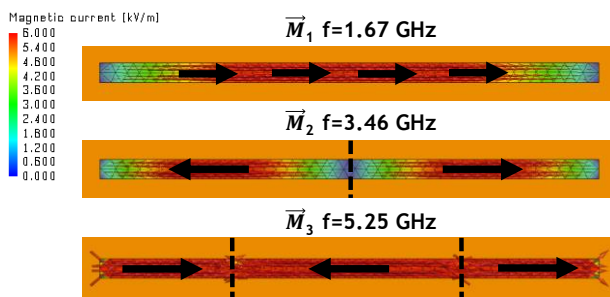


FIGURE 1. Geometry of a rectangular slot ( $L_s = 82$  mm and  $W = 3$  mm) etched in a ground plane of dimensions  $L_h \times L_v$ .



**FIGURE 2.** Eigenvalue ( $b_n$ ) vs. frequency for the first three magnetic characteristic modes ( $M_n$ ) of a rectangular slot with  $L_S = 82$  mm and  $W = 3$  mm, in an infinite ground plane.



**FIGURE 3.** Current distribution of the first three magnetic characteristic modes ( $M_n$ ) of a rectangular slot with  $L_S = 82$  mm and  $W = 3$  mm, at their resonant frequency, in an infinite ground plane. Dashed lines represent nulls of the current distribution.

The excitation conditions for the magnetic modes of the slot are also similar to those of the electric modes of the planar dipole for a particular feeding position. If a voltage gap is inserted in the center of the slot, only the magnetic modes with non-zero magnetic current amplitude at the feeding position and even current distribution, such as  $M_1$  or  $M_3$ , will be excited.

However, a true duality between the slot and the dipole only occurs when an infinite ground plane is considered. In practice, slots are etched in finite conducting planes, and the interaction between the slot modes and the finite metallic ground plane modes must be taken into account. As demonstrated in the following sections, the ground plane size plays an important role in the operating behavior of the slot antenna.

When broadband behavior and pattern stability are desired, an optimum choice of the slot and the ground plane dimensions should be made, in order to properly combine the magnetic resonances of the slot modes and the electric resonances of the ground plane modes.

### III. SLOT EMBEDDED IN A FINITE GROUND PLANE

Fig. 4 shows simulated results for the imaginary part of the input impedance of the rectangular slot structure shown in Fig. 1 ( $L_S = 82$  mm and  $W = 3$  mm) within a ground plane of  $160$  mm x  $160$  mm ( $L_H=L_V=160$  mm). In this case, the antenna is fed by a voltage gap placed at the center of the slot. Simulations have been carried out with the commercial electromagnetic software CST Microwave Studio 2017. As observed, the input impedance exhibits a resonance (R) at  $2.68$  GHz and two anti-resonances at  $1.72$  GHz ( $AR_1$ ) and  $5.36$  GHz ( $AR_2$ ).

As explained before, the inclusion of a voltage gap at the center of the slot prevents the excitation of magnetic CM having a null in their magnetic current amplitude at the feeding position (i.e.  $M_2$ ). As shown in Fig. 4, the anti-resonances (parallel resonances) of the input impedance correspond to the resonances of the magnetic CM  $M_1$  and  $M_3$ , already depicted in Fig. 3. A small deviation in frequency exists due to the effect of the finite ground plane size. As depicted in Fig.4, magnetic mode  $M_1$  is dominant and responsible for the slot radiation until the first resonance that occurs at  $2.68$  GHz (blue area) and magnetic mode  $M_3$  above this frequency (yellow area). The resonance at  $2.68$  GHz can be considered as the frequency at which the transition from mode  $M_1$  to mode  $M_3$  occurs. This resonance occurs when the length of the slot ( $L_S$ ) is close to  $3\lambda/4$ . Usually, this first resonance is the best suited when broadband behavior is desired, since lower values of input resistance are obtained.

For open slot structures, the position of resonances in the input impedance depends on the amplitude and distance between two consecutive anti-resonances. If dimensions of the finite ground plane are modified in order to identify its effect on the position of these resonances and anti-resonances, the results shown in Fig. 5 are obtained. This figure compares the input impedance obtained for different square ground plane sizes, ranging from  $160$  mm x  $160$  mm to  $85$  mm x  $85$  mm. In all cases, the length and width of the slot are the same as in previous sections ( $L_S = 82$  mm and  $W = 3$  mm). As depicted in the figure, changes in ground plane dimensions lead to a minor shift of the anti-resonance frequencies and, particularly, to a certain modification of the real and imaginary parts of the impedance. Consequently, the resonant frequency of the input impedance varies slightly with the size of the ground plane.

However, the dimensions of the ground plane have a much stronger influence on the radiating pattern of the antenna as demonstrated in Fig. 6. When a large ground plane ( $160$  mm x  $160$  mm) is used as in Fig. 6 (a), the radiation pattern degrades with frequency, reducing its stability. In contrast, if a smaller ground plane is used ( $85$  mm x  $85$  mm), radiation pattern properties are better preserved, showing a better stability with higher frequencies, as shown in Fig. 6 (b).

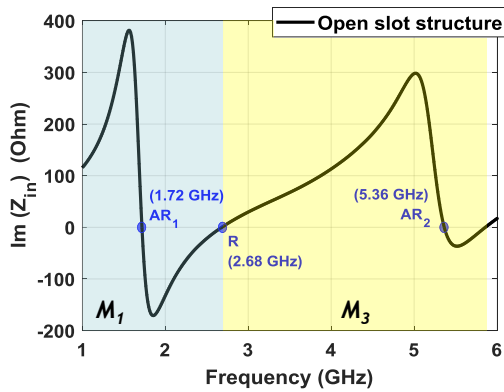


FIGURE 4. Simulated imaginary part of the input impedance of the open slot structure:  $L_s = 82$  mm,  $W = 3$  mm, with a ground plane of 160 mm x 160 mm and 0.35 mm thickness.

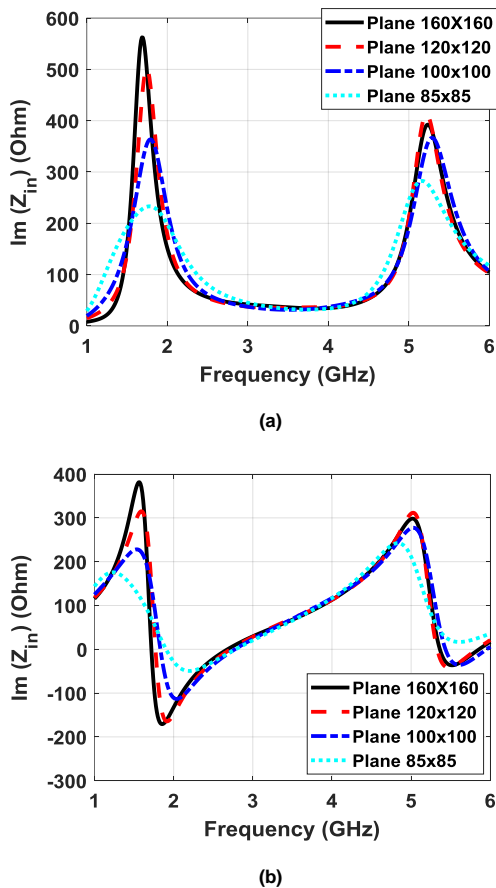


FIGURE 5. Input impedance of the open slot structure:  $L_s = 82$  mm,  $W = 3$  mm, with different ground plane sizes (in mm): (a) Real part; (b) Imaginary part. Thickness of metal is 0.35 mm.

#### IV. DESIGN OF SLOT ANTENNAS IN FINITE GROUND PLANES USING CHARACTERISTIC MODES

In contrast to the complex and quite time-consuming traditional analysis of electric modes associated to the finite-sized ground plane with a slot, this section proposes an alternative simpler method for the analysis, which consists in the combination of both purely electric and magnetic CM.

#### A. TRADITIONAL ANALYSIS WITH ELECTRIC CHARACTERISTIC MODES

A first approach for the analysis of a finite ground plane with an embedded slot or aperture would be focused on the electrical CM of the structure formed by the finite ground plane and the slot [31]-[35].

In this case, the CM of the slotted ground plane will be those associated to the ground plane, but perturbed by the presence of the slot [35], due to the meandering effect produced by the slot on the vertical current modes of the ground plane. It is important to note that the inclusion of the slot in the center of the ground plane does not result in the apparition of new modes or extra resonances. Consequently, the resonances of the magnetic modes of the slot found in Section II are not reflected by this electric modal analysis. The magnetic current modes ( $M_n$ ) of the slot project in equivalent electric current modes around the contour of the slot that couple with the current modes of the metallic plate that share similar current distribution. Thus, the modes of the slot do not appear as independent current modes, but they project on the current modes of the metallic plate. Therefore, information on the slot resonance remains concealed when only an electric modal analysis of the open slot structure is performed.

Let us consider the structure shown in Fig. 1 with a ground plane of 160 mm x 160 mm ( $L_h=L_v=160$  mm). Fig. 7 shows the characteristic angle of the electrical CM ( $J_n$ ) of the slotted structure when excited with a voltage gap at the center of the slot. For the sake of simplicity, only the CM excitable within the considered frequency range have been included. Position of the first resonance of the antenna (2.68 GHz according to Fig. 4) is marked with a dotted blue line in the figure.

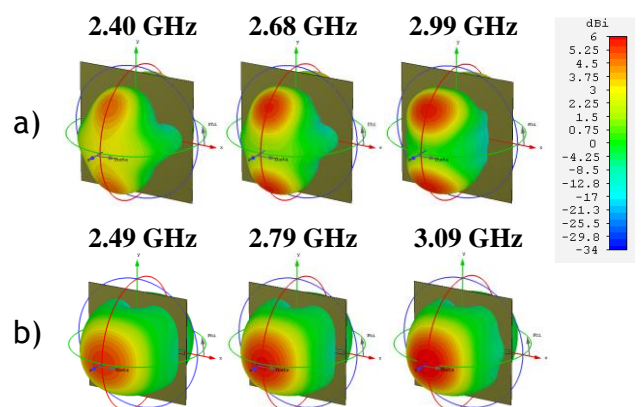
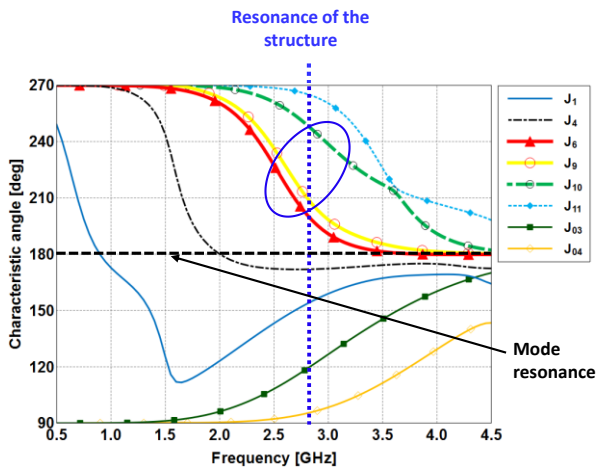


FIGURE 6. Simulated 3D radiation patterns of an open slot antenna with  $L_s = 82$  mm and  $W = 3$  mm: (a) with ground plane of 160 mm x 160 mm; (b) with ground plane of 85 mm x 85 mm.



**FIGURE 7.** Electric CM ( $J_n$ ) involved in the radiation of the open slot antenna shown in Fig. 1, with  $L_h=L_v=160$  mm, when fed with a voltage gap placed at the center of the slot. Position of the first resonance of the antenna (2.68 GHz) is marked with a dotted blue line. CM responsible of the radiation at the resonance frequency of the structure are circled.

As shown, several modes are excited due to the large size of the ground plane and it is observed that electric mode  $J_1$  (fundamental vertical current mode) and mode  $J_4$  (higher order mode) of the slotted ground plane resonate (i.e. their characteristic angle is equal to  $180^\circ$  [5]) before the resonance frequency of the structure at 2.68 GHz. So these modes contribute to the radiation only at lower frequencies. At the resonance frequency of the antenna, only higher order modes  $J_6$ ,  $J_9$  and  $J_{10}$  (which are encircled in Fig. 7) contribute to the radiated power. A power contribution of 25%, 50% and 25% has been computed at 2.68 GHz for each one of these modes, respectively.

Nevertheless, as observed in Fig. 7, the CM excited at the resonance of the structure (2.68 GHz) are far away from their respective mode resonances (3.68 GHz for  $J_6$ , 5.03 GHz for  $J_9$ , and 5.55 GHz for  $J_{10}$ ). Thus, the first resonance of the antenna (2.68 GHz) cannot be linked either to the resonance of any electric mode  $J_n$  associated to the slotted ground plane or to the combination of inductive and capacitive modes. In contrast, several electric modes ( $J_n$ ) of the open slot antenna are excited as a result of the applied voltage gap and the ground plane dimensions, making it very difficult to predict the resonance frequency and the radiation pattern of the antenna.

Consequently, analysis of this antenna based only on electric CM is not a suitable choice for a systematic design, since it fails to provide information about the appropriate excitation or combination of modes and to anticipate resonance frequencies of the structure.

### B. COMBINATION OF PURELY MAGNETIC AND ELECTRIC CHARACTERISTIC MODES

In this section, a new method is proposed for the analysis of slot antennas etched in finite ground planes, by combining

purely magnetic CM of a slot ( $M_n$ ) with electric CM of a finite ground plane ( $J_n$ ) without slot. The aim behind this is to determine the degree of excitation of the electric CM of the finite ground plane, and their contribution to the total radiation pattern of the antenna.

As is well known, the operation of a rectangular slot or aperture embedded in a finite ground plane can be analyzed using equivalent magnetic currents  $M$ , as depicted in Fig. 8. This way, the slot can be replaced by equivalent magnetic currents impressed on an unslotted square ground plane, with the same dimensions as the ground plane of the original slotted antenna. The degree of excitation of the electric CM of the square ground plane ( $J_n$ ) will depend on the coupling between the magnetic currents of the slot and the electric CM of the finite ground plane.

Fig. 9 shows the characteristic angle associated to the electric CM of an unslotted square plate of 160 mm x 160 mm, in free space. As observed, the resonance of the first two electric degenerated modes ( $J_1$ - $J_1'$ ) of the square metallic plate occurs when the length of the ground plane ( $L_h = L_v$ ) is approximately  $\lambda/2$  ( $f = 0.937$  GHz). The current distribution associated to the CM of the square ground plane can be found in [5].

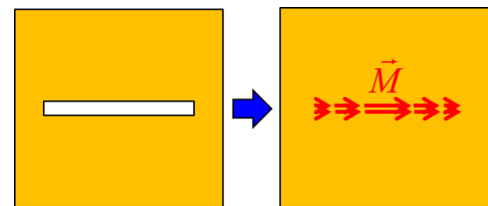


**FIGURE 8.** Model for the analysis of slotted antennas using equivalent magnetic currents.

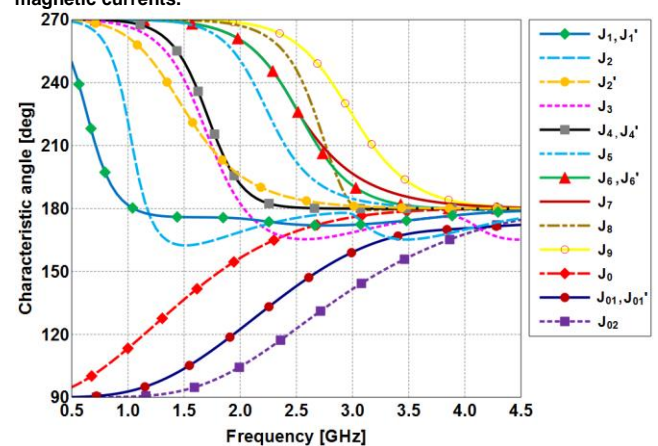


**FIGURE 9.** Characteristic angle vs. frequency for the most relevant characteristic modes of the square plate of length  $L_v = L_h = 160$  mm, without slot.

As shown in Sections II and III, the position of the source on the slot will determine the magnetic CM ( $M_n$ ) that will be excited, which at the same time will couple to different electric CM ( $J_n$ ) in the ground plane. The correlation between

the total radiated far field of the slotted antenna excited at the center of the slot and the modal far field of the  $n^{\text{th}}$  CM of the square ground plane (without slot) ( $J_n$ ) can be used as a measure of how strong modes  $J_n$  are excited. In [41] it was shown that this modal correlation can be expressed as:

$$\rho_{total,n} = \frac{\frac{1}{2Z_0} \iint_{S' \rightarrow \infty} \vec{E}_{total} \cdot \vec{E}_n^* dS}{\sqrt{\frac{1}{2Z_0} \iint_{S' \rightarrow \infty} |\vec{E}_{total}|^2 dS} \sqrt{\frac{1}{2Z_0} \iint_{S' \rightarrow \infty} |\vec{E}_n|^2 dS}} = \frac{a_n}{\sqrt{P_{rad}}} = b_n \quad (3)$$

where  $\vec{E}_{total}$  is the total electric far field,  $\vec{E}_n$  is the electric far field of the  $n^{\text{th}}$  electrical mode,  $Z_0$  is the wave impedance in free space,  $a_n$  represents the weighting coefficient of the  $n^{\text{th}}$  electrical mode [3] and  $b_n$  is the normalized coefficient. The term  $|b_n|^2$  is equal to the percentage each mode contributes to the total radiation power  $P$  [41]:

$$P = \sum_n |b_n|^2 \quad (4)$$

If the total radiated power is normalized to  $P_{rad}$ , the summation of the squared weighting coefficients of the modes will be equal to one.

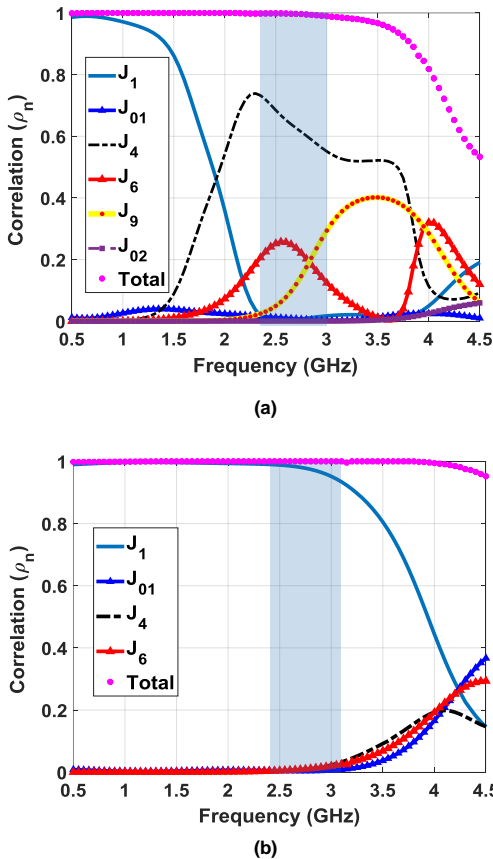


FIGURE 10. Simulated correlation of the total radiation pattern of the proposed slot antenna ( $L_s = 82$  mm and  $W = 3$  mm) versus the finite metallic plane electric CM: (a) Ground plane of 160 mm x 160 mm; (b) Ground plane of 85 mm x 85 mm.

Fig. 10 shows the correlation of the total radiated far field of a slot antenna with  $L_s = 82$  mm and  $W = 3$  mm and two different ground plane dimensions (160 mm x 160 mm and 85 mm x 85 mm, respectively) with the electric CM of the corresponding unslotted ground plane. The shaded area corresponds to the operating bandwidth of the resulting open slot antenna. In this shaded area it is possible to determine the number of ground plane modes involved in the radiation.

As can be seen in Fig. 10 (a), for ground planes with large dimensions (e.g. 160 x 160 mm) the first mode of the ground plane (vertical mode  $J_1$ ) does not contribute to the radiation of the antenna in the operating band, whereas several higher order modes, such as  $J_4$ ,  $J_6$  and  $J_9$  (see Fig. 9), are involved in the radiation. The excitation of various higher order modes in the ground plane at the operating band consequently decreases the stability of the radiation pattern, as was shown in Fig. 6 (a).

However, when a smaller ground plane is considered (e.g. 85 mm x 85 mm), the number of excited modes is reduced. As it is well known, the resonance of the CM associated to this smaller ground plane shifts up in frequency with respect to a larger ground plane, what consequently reduces the number of modes coupled to the ground plane. As shown in Fig. 10 (b), and in contrast to previous case, the antenna radiation is now mostly due to the first mode of the ground plane (vertical current mode  $J_1$ ). As a result, a more stable radiation pattern is achieved, as depicted in Fig. 6 (b).

Therefore, although the ground plane size has a moderate effect on the position of the resonances of the slot antenna embedded in a finite ground plane (see Section III), it has a truly remarkable influence on the stability of the resultant radiation pattern.

Consequently, in order to increase the radiation pattern stability, the ground plane size must be designed to minimize the existence of higher order modes, which create an important diffraction effect in the edges of the ground plane and hence ruin the radiation pattern. The optimum size for the ground plane must be chosen so as to force the fundamental mode of the ground plane ( $J_1$ ) to be the main responsible of radiation in the operating bandwidth.

### C. DESIGN GUIDELINES FOR THE GROUND PLANE SIZE OF A CENTER-FED SLOT ANTENNA

As shown in the previous section, to ensure a stable radiation pattern, the fundamental vertical mode of the ground plane  $J_1$  (resonating with  $L_g \approx \lambda/2$ , see Fig. 1) must be the main contributor to the radiation in the operating bandwidth.

Moreover, the full-wave analysis presented in Section III has demonstrated that the first resonance of the slot (occurring when  $L_s \approx 3\lambda/4$ ) must be chosen when broadband behavior is desired, due to the soft variation exhibited by the input impedance.

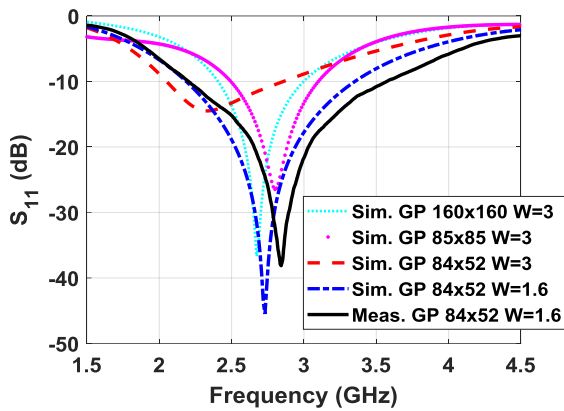


FIGURE 11. Simulated reflection coefficient (dB) for different ground plane (GP) sizes and slot width, and measured reflection coefficient (dB) for the proposed open slot antenna (GP of 84 mm x 52 mm, and  $W = 1.6$  mm).

Logically, if we want to combine these two desirable features in a single antenna, the resonance of the vertical current mode  $J_1$  of the finite ground plane should be as close as possible to the first resonance of the slot. Therefore, the vertical dimension of the ground plane should be  $L_v = 2L_s/3$ .

Taking into account that the minimum horizontal dimension of the ground plane ( $L_h$ ) is determined by the length of the slot ( $L_s$ ), a rectangular ground plane seems to be the most compact solution to achieve the desired radiating behaviour.

To sum up, by considering the results presented in previous sections, the following design principles for the centre-fed rectangular slot antenna (shown in Fig. 1) have been established:

- The horizontal dimension of the ground plane ( $L_h$ ) should be close to the slot length ( $L_s$ ).
- The vertical dimension of the ground plane should be  $L_v = 2L_s/3$ , if a wide impedance bandwidth combined with a stable radiation pattern is desired.

For the slotted antenna under consideration, with a slot length  $L_s = 82$  mm and a central operating frequency at 2.68 GHz, the optimum values for the ground plane correspond to  $L_h = 84$  mm and  $L_v = 52$  mm.

## V. BROADBAND OPEN SLOT ANTENNA DESIGN

Fig. 11 shows the simulated reflection coefficient for the antenna shown in Fig. 1, for the different ground plane sizes considered throughout the paper. Table I summarizes the frequency range and relative bandwidth achieved for the different cases. Accordingly, the antenna designed on the basis of the principles proposed in Section IV.C (with a ground plane of 84 mm x 52 mm, and  $W = 3$  mm) presents an increase above 10% of the relative bandwidth with respect to larger ground planes. By further optimizing the slot width ( $W$ ) to 1.6 mm, an improved match for the input impedance can be obtained, leading to an increased bandwidth of 42.52%, as seen in Table I.

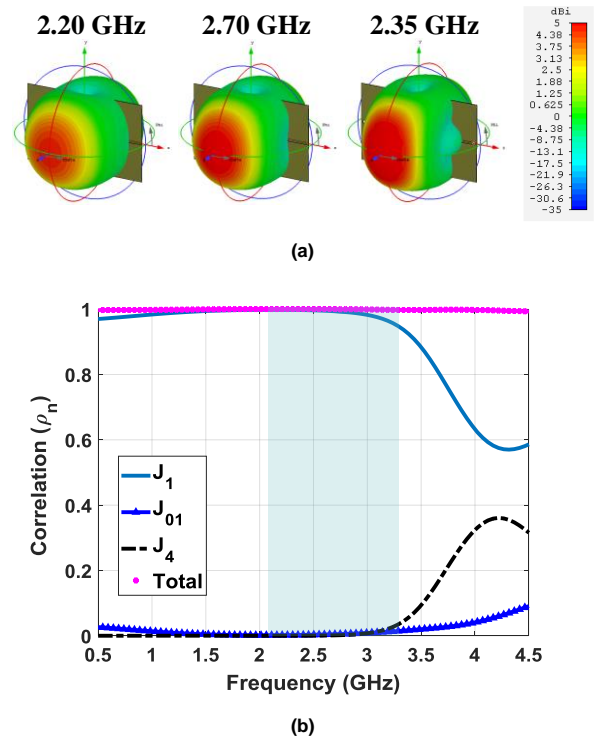


FIGURE 12. Results for the open slot antenna with  $L_s = 82$  mm,  $W = 1.6$  mm and a ground plane of 84 mm x 52 mm: (a) 3D radiation patterns; (b) Simulated correlation of the total radiation pattern of the proposed slot antenna versus the finite ground plane electric CM.

TABLE I  
BANDWIDTH ACHIEVED FOR DIFFERENT GROUND PLANE SIZES

Ground Plane Size ( $L_h \times L_v$ )	Operating Frequency Range	BW (%)	Slot Width (W)*
160x160	2.4 GHz- 2.99 GHz	21.89	3
85x85	2.49 GHz- 3.09 GHz	21.50	3
84x52	2.05 GHz- 2.85 GHz	32.65	3
84x52	2.18 GHz- 3.358 GHz	42.52	1.6

\*Length of the slot is  $L_s = 82$  mm for all cases.

As can be observed in Fig. 12 (a), besides the significant improvement obtained in the bandwidth, the proposed antenna exhibits a greater stability in the radiation pattern within the operation bandwidth, when compared to the results obtained in Fig. 6. The correlation for the proposed antenna with  $W = 1.6$  mm is presented in Fig. 12 (b), showing a substantial reduction of the number of electric CM excited in the ground plane. As predicted, with the selected ground plane size the fundamental vertical mode ( $J_1$ ) of the ground plane is the sole responsible for the antenna radiation. This condition favors the radiation pattern stability observed in Fig. 12 (a).

A prototype for the proposed open slot antenna has been fabricated and measurements have been performed in order to validate the design procedure and the simulated results.



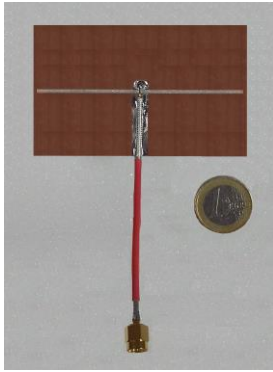


**FIGURE 13.** Manufactured antenna prototype (plane of 84 mm x 52 mm, slot  $W = 1.6$  mm and  $L_s = 82$  mm).

The proposed open slot antenna has been etched on a copper sheet with a thickness of 0.35 mm and dimensions of 84 mm x 52 mm. Fig. 13 shows the manufactured antenna prototype, fed by a 50  $\Omega$  coaxial cable.

A comparison of the simulated and measured S-parameter of the antenna prototype is displayed in Fig. 11. As can be observed, the measured -10 dB impedance bandwidth ranges from 2.2 GHz to 3.57 GHz, corresponding to a 47.48% relative bandwidth. This represents an increment above 5% with respect to the simulated results.

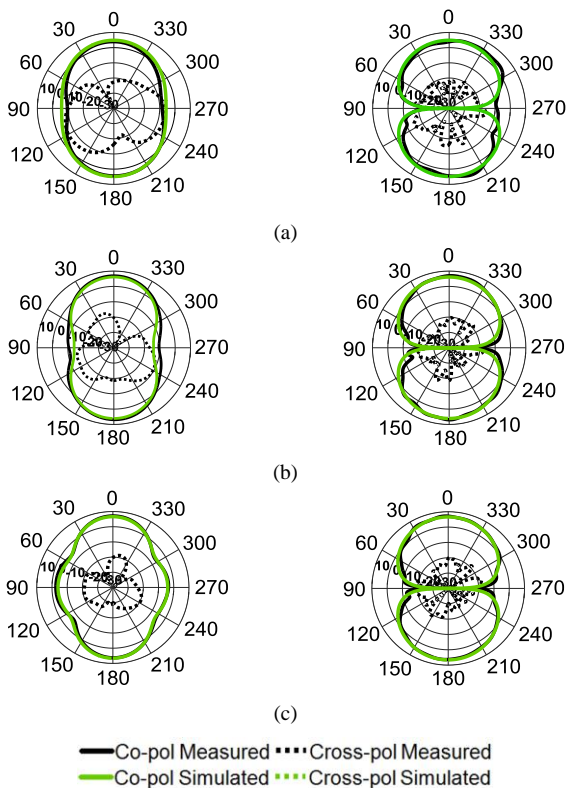


**FIGURE 14.** Simulated and measured radiation patterns (directivity) for proposed antenna at three frequencies within the operating bandwidth: (a) 2.21 GHz. (b) 3 GHz. (c) 3.55 GHz.

Fig. 14 shows the simulated and measured 2D radiation patterns at XZ and YZ planes for the proposed antenna prototype, within the operating frequency. As shown, both patterns agree well. However, the measured cross-polarization level for the lower frequencies (under 2.4 GHz) is slightly higher than simulated (below -40 dBi for all frequencies), mainly due to the parasitic radiation of the feeding cable. Furthermore, the radiation pattern is rather stable within the whole operating bandwidth.

The peak gain and the radiation efficiency have been measured, reaching values up to 6.7 dB and 96%, respectively.

Finally, Table II shows a comparison in terms of total size, bandwidth and gain of the proposed antenna with respect to very recent and relevant works reported in [42]-[46]. As observed, this very simple antenna presents a better -10 dB bandwidth with a total smaller size compared to the referenced works, along with a higher gain and efficiency. Moreover, another of the benefits is that it maintains the same impedance and radiation bandwidth operating range.

TABLE II  
COMPARISON WITH RECENT DESIGNS

References	ANTENNA SIZE* ( $\lambda$ )	Total Area* ( $\lambda^2$ )	BW (%)	Gain (dB)
Ref [42]	1.14 x 0.57	0.65	20.40	-
Ref [43]	1.37 x 1.37	1.87	32.70	4
Ref [44]	0.74 x 1.38	1.02	5.4	-
Ref [45]	1.12 x 0.87	0.97	46.1	6.8
Ref [46]	0.15 x 0.18	0.027	0.95	3.6
<b>Proposed Antenna</b>	<b>0.8x0.5</b>	<b>0.4</b>	<b>47.48</b>	<b>6.7</b>

\* $\lambda$  is the wavelength at the central frequency of the operating band.

## VI. CONCLUSIONS

Narrow-in-width open slot antennas embedded in a finite ground plane have been analyzed using the TCM, with the aim to offer some guidelines for their design and to provide a physical understanding of the interaction between the magnetic modes of the slot and the electric modes of the finite metallic ground plane.

On the one hand, magnetic modes of a slot etched in an infinite plane have been obtained using the magnetic formulation of TCM. It has been demonstrated that when a voltage gap is applied at the center of the slot, the resonances of the magnetic modes determine the anti-resonances of the input impedance of the slotted antenna. In turn, the resonance frequencies of the input impedance depend on the amplitude and the distance between two consecutive anti-resonances. In narrow-in-width slots, the first resonance occurs when the length of the slot is close to  $3\lambda/4$ .

On the other hand, the electric formulation of TCM applied to the open slot in a finite metallic plane has revealed that the excitation of the electric modes of the ground plane have little effect on the input impedance of the antenna, but have a truly remarkable influence on the radiation pattern

behavior and stability. It has been demonstrated that the reduction of the ground plane size reduces the number of ground plane modes involved in the radiation of the antenna, leading in turn to an improvement in the stability of the radiation pattern due to an improved coupling between the slot and the fundamental vertical mode of the finite ground plane.

A systematic design procedure based on the combination of both electric and magnetic characteristic modes has been proposed, together with some guidelines for the optimization of center-fed slotted antennas, in order to get wide impedance bandwidth and stability of the radiation pattern. It is worth to remark that the proposed method can be extended to other type of excitation, like off-centered slots or double-fed slots.

Simulations and measurements of a compact narrow-in-width wideband open slot antenna have been presented as an example of the design and optimization procedure. An impedance bandwidth of 47.48% has been achieved with the proposed antenna, with a very stable radiation pattern.

Finally, it is worth to remark that for applications requiring the use of very large platforms or ground planes, the proposed antenna can be easily integrated by creating a slotted frame around the antenna, which does not alter its performance.

## References

- [1] R. J. Garbacz, "A generalized expansion for radiated and scattered fields," Ph.D. dissertation, Ohio State Univ., Columbus, OH, USA, 1968.
- [2] R. F. Harrington and J. R. Mautz, "Theory of characteristic modes for conducting bodies," *IEEE Trans. Antennas Propagat.*, vol. AP-19, no. 5, pp. 622-628, September 1971.
- [3] R. F. Harrington and J. R. Mautz, "Computation of characteristic modes for conducting bodies," *IEEE Trans. Antennas Propagat.*, vol. AP-19, no. 5, pp. 629-639, September. 1971.
- [4] M. Cabedo-Fabres, E. Antonino-Daviu, A. Valero-Nogueira, and M. F. Bataller, "The Theory of Characteristic Modes revisited: A contribution to the design of antennas for modern applications," *IEEE Antennas Propag. Mag.*, vol. 49, no. 5, pp. 52-68, Oct. 2007.
- [5] M. Cabedo-Fabrés, "Systematic design of antennas using the Theory of Characteristic Modes," Ph.D. dissertation, Dept. Commun., Polytechn. Univ. Valencia, Valencia, Spain, Feb. 2007.
- [6] J. J. Adams, and J. T. Bernhard, "A modal approach to tuning and bandwidth enhancement of an electrically small antenna," *IEEE Trans. on Antennas and Propagat.*, vol. 59, no. 4, pp. 1085-1092, 2011.
- [7] N. L. Bohannon; J.T. Bernhard, "Design guidelines using characteristic mode theory for improving the bandwidth of PIFAs," *IEEE Trans. on Antennas and Propagat.*, vol. 63, no. 2, pp. 459 - 465, 2015.
- [8] B.A. Austin and K.P. Murray, "The application of characteristic-mode techniques to vehicle-mounted NVIS antennas," *IEEE Antennas and Propagat. Magazine*, vol. 40, no. 1, pp. 7-21, 1998.
- [9] J. Chalas, K. Sertel, J. L. Volakis, "NVIS synthesis for electrically small aircraft using characteristic modes," *IEEE Antennas and Propagat. Society Int. Symp.*, pp. 1431-1432, 2014.
- [10] E. Antonino-Daviu, M. Cabedo-Fabrés, M. Ferrando-Bataller, and J. I. Herranz-Herruzo, "Analysis of the coupled chassis-antenna modes in mobile handsets," *IEEE Antennas and Propagat. Society Int. Symp.*, vol. 3, pp. 2751-2754, 2004.
- [11] J. Ethier, E. Lanoue, and D. McNamara, "MIMO handheld antenna design approach using characteristic mode concepts," *Microwave and Optical Tech. Letters*, vol. 50, no. 7, pp. 1724-1727, July 2008.
- [12] M. Sonkki, M. Cabedo-Fabrés, E. Antonino-Daviu, M. Ferrando-Bataller, and E.T. Salonen, "Creation of a Magnetic Boundary Condition in a Radiating Ground Plane to Excite Antenna Modes," *IEEE Trans. Antennas Propagat.*, vol. 59, no. 10, pp. 3579- 3587, Oct. 2011.
- [13] L. Qu, H. Lee, H. Shin, M.-G. Kim, H. Kim, "MIMO antennas using controlled orthogonal characteristic modes by metal rims," *IET Microwaves, Antennas & Propagation*, vol. 11, no. 7, pp. 1009-1015. 2017.
- [14] D. Wen, Y. Hao, H. Wang, H. Zhou, "Design of a wideband antenna with stable omnidirectional radiation pattern using the Theory of Characteristic Modes," *IEEE Trans. Antennas Propagat.*, vol. 65, pp. 2671-2676, May 2017.
- [15] R.F.Harrington, J.R.Mautz and Y.Chang, "Characteristic modes for dielectric and magnetic bodies," *IEEE Trans. Antennas Propagat.*, vol. 20, pp.194-198, 1972.
- [16] T. Bernabeu-Jiménez, A. Valero-Nogueira, F. Vico-Bondia, E. Antonino-Daviu, M. Cabedo-Fabrés, "A 60 GHz LTCC rectangular dielectric resonator antenna design with characteristic modes theory," *IEEE Antennas and Propagat. Society Int. Symp.*, pp. 1928-1929, 2014.
- [17] P. Yla-Oijala, D. C. Tzarouchis, E. Raninen, A. Sihvola, "Characteristic Mode Analysis of Plasmonic Nanoantennas," *IEEE Trans. Antennas Propagat.*, vol. 65, pp. 2165-2172, May 2017.
- [18] A. Adam Salih, Z. N. Chen, K. Mouthaan, "Characteristic mode analysis and metasurface-based suppression of higher order modes of a 2x2 closely spaced phased array," *IEEE Trans. Antennas Propagat.*, vol. 65, pp. 1141-1150, March 2017.
- [19] F. H. Lin, Z. N. Chen, "Low-profile wideband metasurface antennas using characteristic mode analysis," *IEEE Transactions on Antennas and Propagation*, vol. 65, pp. 1706-1713. April 2017.
- [20] R.F. Harrington and J. R. Mautz "Characteristic modes for aperture problems," *IEEE Transactions on Microwave Theory and Techniques*, vol. MTT-33, no.6, pp. 500-505, June 1985.
- [21] K.Y. Kabalan, R.F. Harrington, H. A. Auda, and J. R. Mautz, "Characteristic modes for slots in a conducting plane, TE case," *IEEE Transactions on Antennas and Propagation*, vol. AP-35, no. 2, pp.162-168, Feb. 1987.
- [22] K.Y. Kabalan, R.F. Harrington, J. R. Mautz and H. A. Auda, "Characteristic modes for slots in a conducting plane, TM case," *IEEE Trans. Antennas and Propagat.*, vol. AP-35, no. 3, pp. 331-335, March. 1987.
- [23] E. Antonino-Daviu, "Analysis and design of antennas for wireless communications using modal methods," Ph.D. dissertation, Dept. Commun., Polytechn. Univ. Valencia, Valencia, Spain, Feb. 2008.
- [24] A. El-Hajj, and K. Y. Kabalan, "Characteristic modes of a rectangular aperture in a perfectly conducting plane," *IEEE Trans. on Antennas and Propagat.*, vol. 42, no. 10, October 1994.
- [25] R. Azadegan and K. Sarabandi, "A novel approach for miniaturization of slot antennas," *IEEE Trans. Antennas Propagat.*, vol. 51, no. 3, pp. 421-429, Mar. 2003.
- [26] N. Behdad and K. Sarabandi, "A multiresonant single-element wideband slot antenna," *IEEE Antennas Wireless Propagation Letter*, vol. 3, pp. 5-8, 2004.
- [27] W.-J. Lu and L. Zhu, "Wideband stub-loaded slotline antennas under multi-mode resonance operation," *IEEE Trans. Antennas Propagat.*, vol. 63, no. 2, pp. 818-823, Feb. 2015.
- [28] C. J. Wang, M.H. Shih and L. T. Chen, "A Wideband Open-Slot Antenna with Dual-Band Circular Polarization," *IEEE Antennas Wireless Propagation Letter*, vol. 14, pp. 1306-1309, 2015.
- [29] T. Oh, Y.-G. Lim, C.-B. Chae, and Y. Lee, "Dual-polarization slot antenna with high cross-polarization discrimination for indoor small-cell MIMO systems," *IEEE Antennas Wireless Propagation Letter*, vol. 14, pp. 374-377, 2015.
- [30] E. Antonino-Daviu, M. Cabedo-Fabrés, M. Ferrando-Bataller, and V. M. Rodrigo-Peñarrocha, "Modal Analysis and Design of Band-notched UWB Planar Monopole Antennas," *IEEE Trans. Antennas Propagat.*, vol. 58, no. 5, pp. 1457-1467, May 2010
- [31] Y. Chen, and C.F. Wang, "Characteristic-mode-based improvement of circularly polarized U-slot and E-shaped patch antennas," *IEEE Antennas Wireless Propag. Lett.*, vol. 11, pp. 1474-1477, 2012.

- [32] M. Khan, D. Chatterjee, "Characteristic mode analysis of a class of empirical design techniques for probe-fed, U-slot microstrip patch antennas," *IEEE Trans. on Antennas and Propagat.*, vol. 64, pp. 2758–2770, July 2016.
- [33] E. Antonino-Daviu, M. Cabedo-Fabres, M. Sonkki, N. Mohamed Mohamed-Hicho, M. Ferrando-Bataller, "Design guidelines for the excitation of characteristic modes in slotted planar structures," *IEEE Trans. on Antennas and Propagat.*, vol. 64, pp. 5020–5029, Dec. 2016.
- [34] A. Boukarkar, X. Q. Lin, J. W. Yu, P. Mei, J. Yuan, Y. Q. Yu, "A Highly Integrated Independently Tunable Triple-Band Patch Antenna," *IEEE Antennas and Wireless Propag. Letters*. To appear.
- [35] M. Cabedo-Fabrés, A. Valero, E. Antonino-Daviu and M. Ferrando-Bataller, "Modal analysis of a radiating slotted PCB for mobile handsets", in *1st European Conference on Antennas and Propagation (EUCAP)*, pp. 1-6, Nov. 2006.
- [36] Y. Chang and R. Harrington, "A surface formulation for characteristic modes of material bodies," *IEEE Trans. on Antennas and Propagat.*, vol. 25, no. 6, pp. 789–795, 1977.
- [37] Z. T. Miers and B. K. Lau, "Computational Analysis and Verifications of Characteristic Modes in Real Materials," in *IEEE Trans. Antennas Propag.*, vol. 64, no. 7, pp. 2595-2607, July 2016
- [38] S. Huang, J. Pan, Y. Luo, "Investigations of Non-Physical Characteristic Modes of Material Bodies," DOI 10.1109/ACCESS.2018.2818196, *IEEE Access*.
- [39] R. Lian, J. Pan and S. Huang, "Alternative Surface Integral Equation Formulations for Characteristic Modes of Dielectric and Magnetic Bodies", *IEEE Trans. on Antennas and Propagat.*, vol. 65, no. 9, pp. 4706–4716, Sept. 2017.
- [40] T. Bernabeu-Jiménez, A. Valero-Nogueira, F. Vico-Bondia, and Ahmed A. Kishk, "On the Contribution to the Field of the Nonphysical Characteristic Modes in Infinite Dielectric Circular Cylinders Under Normal Excitation," *IEEE Trans. on Antennas and Propagat.*, vol. 66, no. 1, pp. 505–510, 2018.
- [41] Safin, E., Manteuffel, D.: "Reconstruction of the characteristic modes on an antenna based on the radiated far field," *IEEE Trans. Antennas Propag.*, 2013, 61, (6), pp. 2964–2971
- [42] C. K. Chang, W. J. Liao, C. C. Tsai, "Metal Body-Integrated Open-End Slot-Antenna Designs for Handset LTE Uses," *IEEE Trans. Antennas and Propag.*, vol. 64, no.12, pp. 5436- 5440, Dec 2016.
- [43] W.-J. Lu, L. Zhu, "A novel wideband slotline antenna with dual resonances: Principle and design approach", *IEEE Antennas and Wireless Propag. Let.*, vol. 14, pp. 795–798, 2015.
- [44] K. L. Wong, W. C. Wu, "Very-low-profile hybrid open-slot/closed-slot/inverted-F antenna for the LTE smartphone", *Microwave and Optical Tech. Let.*, vol. 58, no. 7, pp. 1572–1577, July 2016.
- [45] H. T. Hu, F. C. Chen, "Novel Broadband Filtering Slotline Antennas Excited by Multimode Resonators", *IEEE Antennas and Wireless Propag. Let.*, vol. 16, pp. 489–492, 2017.
- [46] A. P. Saghati, K. Entesari, "An Ultra-Miniature SIW Cavity-Backed Slot Antenna", *IEEE Antennas and Wireless Propag. Let.*, vol. 16, pp. 313–316, 2017.